Molecular Cell, Vol. 1, 67–78, December, 1997, Copyright ©1997 by Cell Press

Crystal Structure of the Complex of Diphtheria Toxin with an Extracellular Fragment of Its Receptor

Gordon V. Louie, Walter Yang, Marianne E. Bowman, and Senyon Choe*
Structural Biology Laboratory
Salk Institute for Biological Studies
La Jolla, California 92037

Summary

We describe the crystal structure at 2.65 Å resolution of diphtheria toxin (DT) complexed 1:1 with a fragment of its cell-surface receptor, the precursor of heparin-binding epidermal-growth-factor-like growth factor (HBEGF). HBEGF in the complex has the typical EGF-like fold and packs its principal β hairpin against the face of a β sheet in the receptor-binding domain of DT. The interface has a predominantly hydrophobic core, and polar interactions are formed at the periphery. The structure of the complex suggests that part of the membrane anchor of the receptor can interact with a hinge region of DT. The toxin molecule is thereby induced to form an open conformation conducive to membrane insertion. The structure provides a basis for altering the binding specificity of the toxin, and may also serve as a model for other EGF–receptor interactions.

Introduction

Diphtheria toxin (DT) is produced by the bacterium Corynebacterium diphtheriae lysogenized by corynephage β (Collier, 1975). A single molecule of the toxin, a protein of 535 amino acid residues, can be sufficient to kill a cell (Yamaizumi et al., 1978). The killing action of DT involves three distinct steps: (1) binding to a receptor on the surface of sensitive cells and subsequent receptor-mediated endocytosis; (2) translocation of the catalytic domain of the toxin across the endosomal membrane and into the cytoplasm of the cell, a process induced by the acidic environment inside the endosome; and (3) catalytic transfer of an ADP-ribosyl group from NAD^+ to a specific modified histidine on the ribosomal elongation factor 2, thus preventing protein synthesis in the cell and leading to cell death.

The three-dimensional structure of DT (Choe et al., 1992) showed that the three activities of the toxin are performed by distinct structural domains: the receptor-binding (R, residues 387–535), the pore-forming membrane-translocation (T, residues 200–378), and the catalytic (C, residues 1–188) domain. The structures of DT in two different forms, monomeric and dimeric (Bennett and Eisenberg, 1994; Bennett et al., 1994), differ in that the R domain is swung out into an "open conformation" in dimeric DT. As a result, each "swapped" R domain makes little interaction with the C and T domains of its own molecule, but instead associates more closely with these domains of the opposing monomer of the dimer. The large movement of the R domain is effected by a change in conformation of a hinge segment (residues 379–386), which tethers the R domain to the rest of the DT molecule. However, in the monomeric and dimeric forms, the R domain is positioned identically relative to its most closely associated C and T domains, and therefore forms the same interface with the other two domains.

The DT molecule opportunistically binds on the surface of the target cell through the membrane-anchored precursor of heparin-binding epidermal-growth-factor-like growth factor (HBEGF) (Naglich et al., 1992). HBEGF is a protein of 208 amino acid residues and is synthesized primarily by macrophages, but also by vascular endothelial and smooth muscle cells. The primary translation product consists of a signal peptide, a pro sequence, a heparin-binding motif, an EGF-like module, a short linker, a transmembrane anchor, and a small cytoplasmic domain (Higashiyama et al., 1992). Proteolytic processing releases a soluble growth factor, a 75–86 residue fragment bearing only the heparin-binding and EGF-like domains (Higashiyama et al., 1992). The EGF-like growth factor portion of HBEGF (residues 106–147) contains the EGF-typifying six cysteines, which form three disulfide bonds, and is a ligand for the EGF receptor. DT has been shown to bind HBEGF also through the EGF-like domain (Mitamura et al., 1995). The binding affinity is relatively high; the apparent dissociation constant of the DT–HBEGF complex has been estimated to be 10^{-8}–10^{-9} M (Shen et al., 1994; Mitamura et al., 1995). It is notable that binding of DT to HBEGF is highly sequence-specific: human or monkey HBEGF is recognized, whereas the 80% identical (within the EGF module) mouse or rat HBEGF are not (Mitamura et al., 1995).

This paper describes the crystal structure of diphtheria toxin bound to an extracellular fragment of human HBEGF. The structure provides a detailed view of the DT–HBEGF intermolecular interface and identifies key residues from DT involved in complexing HBEGF. This information will provide a basis for designing mutations that will alter the binding specificity of DT toward other EGF-like targets. An attractive goal is to use engineered DTs as therapeutic agents for delivering cytotoxic activity to specific cells. The structure determination of the complex is also an initial step in the study of the translocation of the DT catalytic domain across the endosomal membrane, which occurs after binding of the toxin to the membrane-bound receptor. An improved knowledge of this process will be useful for understanding the efficacy of cytotoxic conjugates of DT with targeting marker proteins (Pastan et al., 1992; Sweeney and Murphy, 1995), and more generally the cellular mechanisms of membrane translocation of proteins.

Results and Discussion

Binding Stoichiometry of DT and HBEGF

Complexation between DT and HBEGF was assessed with methods that exploit the substantial overall charge

*To whom correspondence should be addressed.

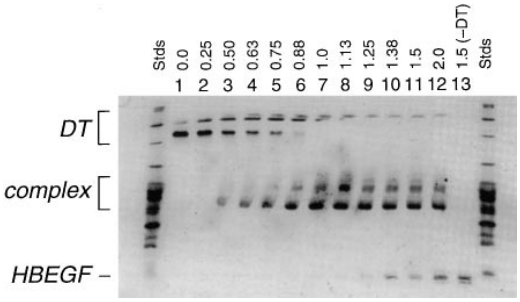

Figure 1. Isoelectric-Focusing Binding Assay of DT and HBEGF

A fixed amount (13.4 μg) of DT was titrated with increasing amounts of HBEGF (0.25–2.0 molar ratio). Uncomplexed DT (lane 1) and HBEGF (lane 13) focus at pI ~5 and pI ~10, respectively, whereas the complexed proteins focus at an intermediate pI. Saturation of HBEGF binding by DT is indicated by the loss of free DT and the appearance of free HBEGF (lanes 7 and 8).

difference between the two proteins (pI DT ~ 5.5, pI HBEGF ~ 10.0). Both isoelectric focusing and native electrophoresis permit the complexed proteins to be separated from the individual components. From experiments in which a fixed amount (known accurately from amino acid analysis) of one of the proteins was titrated with varying amounts of the other, DT and HBEGF were determined to form a complex with 1:1 stoichiometry (Figure 1).

It has been suggested that an oligomer of more than one T domain is required to form the pore assembly capable of translocating a C domain across the endosomal membrane (Zhan et al., 1995; Oh et al., 1996). The present results from the binding experiments and from the crystallographic structure determination (as described below) suggest that just a 1:1 complex of DT with HBEGF provides the building block for such a multimeric association of DT.

General Features of the DT–HBEGF Interaction

The receptor-binding (R) domain of DT consists of an antiparallel β barrel that is somewhat flattened to form two distinct β sheets (see Figure 2B). The β strands have a similar overall topology to that of the immunoglobulin (Ig) domains (Choe et al., 1992); the strands Rβ2, -3, -4, -5, -8, -9, and -10 correspond to the A, B, C, D, E, F, and G strands of the Igs. Like the Ig variable domain, DT's R domain contains an insertion of two β strands with respect to an Ig constant domain. However, the insertion occurs after the fourth strand of the barrel (Rβ5) in DT, rather than after the third (C) as in the Ig variable domain.

The structure of the DT–HBEGF complex (Figure 2A) reveals that the crescent-shaped HBEGF molecule packs against a saddle-shaped crevice in the wall of the β barrel of DT's R domain (Figure 2B). The crevice flanks the face of the β sheet containing the strands Rβ6, -7, -4, -9, and -10. The loop connecting the latter two strands, which was earlier predicted to participate in receptor recognition (Shen et al., 1994), forms a large part of the lower wall of the crevice (as viewed in Figure 2B). The EGF module of HBEGF consists largely of a β hairpin, which in the complex contributes the third sheet to a three-layered β sandwich. In this sandwich, the peptide-bond planes in each β sheet are nearly parallel to those in the adjacent sheet. The β strands in each sheet cross at an angle of approximately −40° with respect to strands in the adjacent sheet. The closest approach of α carbons in the apposed β sheets of the two molecules is about 8–9 Å. It is notable that the close association of the major β hairpin of HBEGF with a β sheet from DT shares many features with the intramolecular interaction between the EGF and fibronectin-like modules of tissue-type plasminogen activator (Smith et al., 1995). In t-PA, the same concave face of EGF participates in binding, although the interaction between the apposed β structures is somewhat less extensive.

Although face-to-face packing of β sheets is common within single protein domains (Chothia and Janin, 1981), it is rarely seen between protein molecules. However, intermolecular association of this type does occur frequently with proteins from the Ig superfamily. In particular, in terms of both the intersheet separation distance and β strand crossing angle, the DT–HBEGF interaction bears remarkable similarity to the interaction between two constant (C_{H1}-C_L or C_{H3}-C_{H3}) domains in an Ig molecule (entries 1mco and 8fab in the PDB), or the related interaction between Cα and Cβ domains of the T-cell receptor (Garcia et al., 1996). This similarity is perhaps not unexpected considering the structural similarity between DT's R domain and an Ig domain. In the dimer of Ig constant domains, a four-layered β sandwich is formed, and the saddle-shaped crevice is less curved to accommodate the wider β sheet of the partner constant domain. In comparison to DT's R domain, the Ig constant domains interface through the opposite sheet (ABED) of the β sandwich. However, several cell-adhesion molecules (including CD2, CD8, and VCAM-1) that are members of the Ig superfamily have been shown to use the CFG face of the β sandwich to interact with other adhesion proteins (Jones et al., 1995).

The DT–HBEGF Interface

At the DT–HBEGF interface, each molecule buries approximately 1100 $Å^2$ of surface. For the smaller HBEGF molecule, the buried area represents nearly 50% of the total surface area. Due to the face-to-face association of β sheets at the interface, the main-chain polar groups in each sheet are involved primarily in intrasheet hydrogen bonding. As a result, the central part of the intermolecular interface involves only amino acid side chains and is predominantly nonpolar (Figure 3A). Nonpolar surfaces are formed on DT by the side chains of F389, A430, L433, I464, V468, F470, G510, L512, V523, and F530; and on HBEGF by the side chains of V124, L127, A129, P130, S131, I133, and P136, the G137 backbone, and the C134–C143 disulfide. An exception to the nonpolarity of the core of the interface is the side chain of DT-K526, which is hydrogen-bonded to the carbonyl oxygens of HBEGF-C132 and E141. The majority of the direct hydrogen-bond interactions (17 in total) are formed at the periphery of the interface, and a number

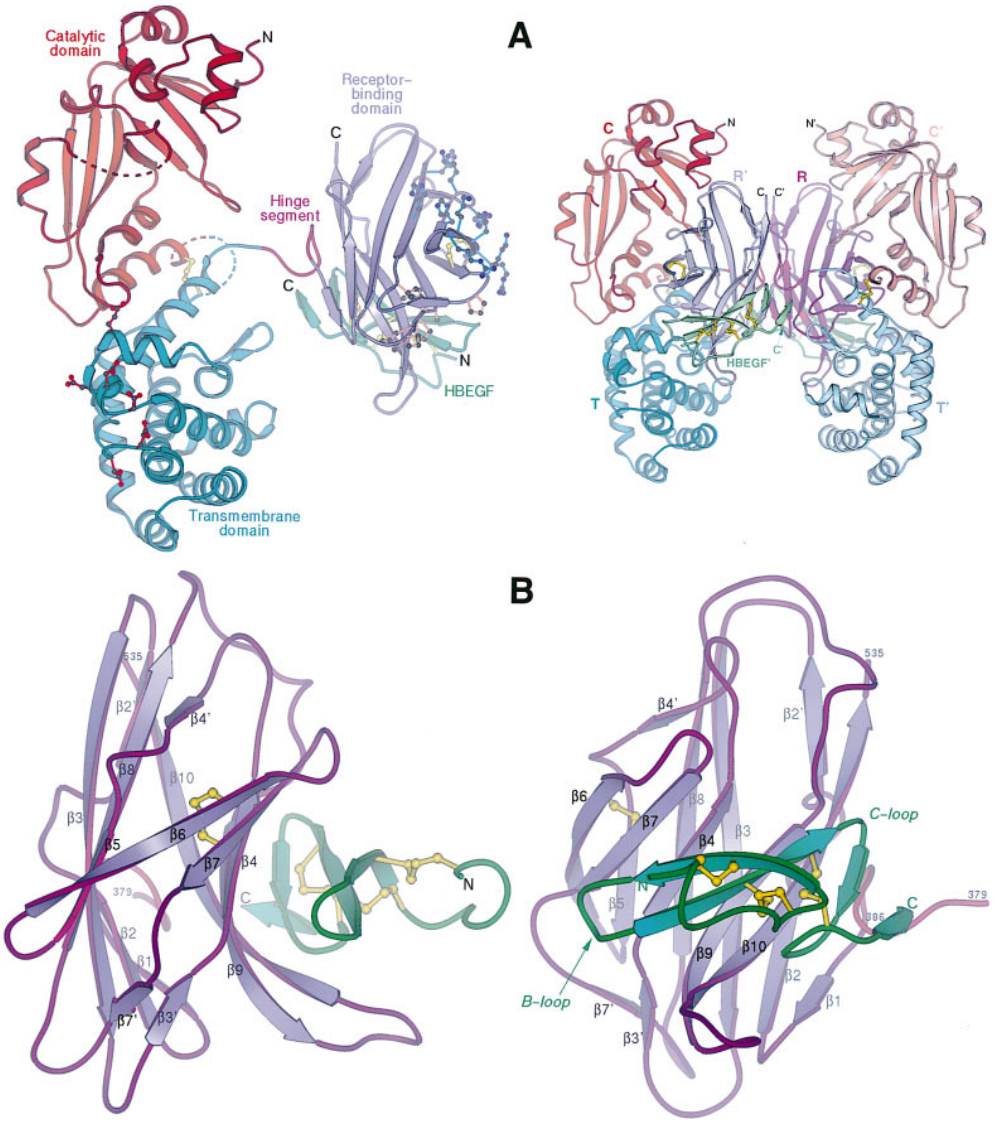

Figure 2. The DT–HBEGF Complex

(A) Overall view of the DT–HBEGF complex. DT's C, T, and R domains are colored red, light blue, and violet, respectively, and the hinge segment (residues 379–386) is colored purple. HBEGF is colored light green. Disulfide bonds are drawn in yellow. Note the "open" conformation of the DT molecule, in which the R domain with its associated HBEGF molecule is swung away from the C and T domains. Three functionally important clusters of side chains on DT are also shown: an acidic (red) cluster on the T domain, and hydrophobic (brown) and basic (blue) clusters on the R domain. Two segments of the DT polypeptide chain that are not visible in electron-density maps (residues 39–44 and 189–199) are dashed. The inset (right) shows the DT–HBEGF complex in the crystallographic dimer, with the three domains of the opposing DT molecule in the dimer labeled C′, T′, and R′ and colored in paler shades of red, blue, and violet. The three domains C-T-R′ or C′-T′-R constitute one closed DT molecule. All molecular images were created with the program Setor (Evans, 1993), except Figure 3B.

(B) Overall view (left side and front) of DT's R domain complexed with HBEGF. β strands are shown as flat arrows, and for the R domain are labeled according to the nomenclature of Bennett et al. (1994). The coloring scheme is the same as that used in (A).

of these involve main-chain polar groups. Additional hydrogen-bond interactions are mediated by bridging water molecules, including two networks of six water molecules occupying cavities adjacent to K526. Particularly notable interactions are formed by the side chain of HBEGF-E141, which bridges two basic side chains of DT, H391 and K516 (Figure 3A). Overall, the interface between the two molecules shows excellent electrostatic and shape complementarity (Figure 3B): there are five intermolecular ion pairs and only the two small cavities (accessible to a probe sphere 1.4 Å in radius) adjacent to DT-K526. These factors together with the direct and water-mediated interactions (Table 1) undoubtedly contribute to the specificity of DT for (the human form of) HBEGF and the relatively tight binding ($K_d \sim 10^{-8}$ M).

Consistent with the modular organization of the DT molecule, HBEGF forms direct contacts with only the R domain. One important implication of this result is that

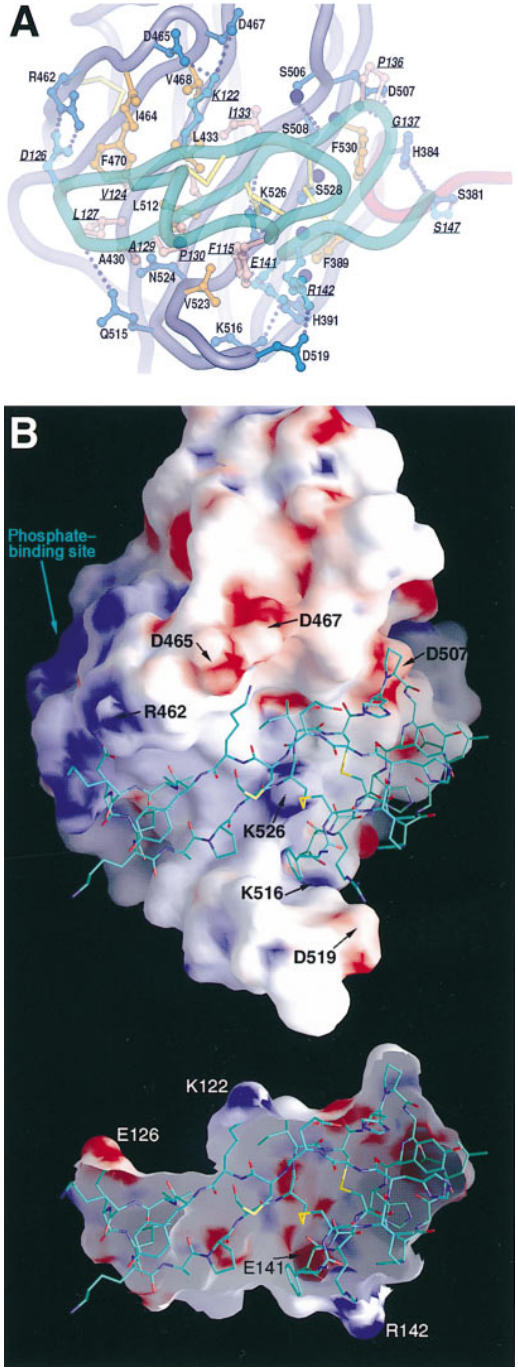

Figure 3. The Interaction between DT's R Domain and HBEGF

(A) Interactions between DT's R domain and HBEGF. The polypeptide-chain backbones of the two molecules are represented as tubes (for clarity, partially transparent for HBEGF), and colored according to the scheme of Figure 2A. Nonpolar side chains at the interface are drawn in orange (DT) and brown-orange (HBEGF); polar side chains are drawn in blue (DT, darker; HBEGF, lighter). Direct intermolecular hydrogen-bond or salt-bridge interactions are shown as dark-blue dotted lines. Six water molecules that form bridging interactions between DT and HBEGF are also drawn as dark blue spheres. Amino acid residue labels use the one-letter abbreviation and are italicized and underlined for HBEGF.

(B) Complementarity of interacting surfaces between DT's R domain (top) and HBEGF (bottom). Electrostatic potentials (positive, blue; negative, red) were calculated assuming a salt concentration of 0.15 M, and with full charges on aspartate, glutamate, lysine, and arginine side chain groups, and partial charges on backbone polar atoms (N, −0.2, H_N, +0.2; C, +0.4; O, −0.4). For clarity, the front (distal to DT) portion of the HBEGF surface has been removed. The atomic skeleton of HBEGF is superimposed on both surfaces, and colored according to atom type (nitrogen, blue; oxygen, red; carbon, green). On each molecular surface, the position of key charged groups that participate in intermolecular ion-pair interactions (see Table 1) are labeled. A cluster of basic side chains on the back face of DT's R domain is evident as a dark blue patch. (Calculated and displayed with the program GRASP [Nicholls et al., 1991].)

Table 1. Interactions between DT and HBEGF in the Complex

Hydrogen Bond and Salt Bridge		
DT Atom	HBEGF atom	Distance (Å)
S381 OG	S147 OG	2.7
H384 NE2	S147 OT1	3.0
H384 NE2	S147 OT2	3.7
H391 NE2	E141 OE1	2.8
R462 NE	E126 OE1	2.9
R462 NH2	E126 OE2	2.8
D465 OD2	K122 NZ	2.7
D467 OD2	K122 NZ	3.7
S506 OG	C134 O	2.7
D507 OD1	G137 N	3.0
D507 OD2	G137 N	3.3
Q515 NE2	L127 O	3.3
K516 NZ	E141 OE2	3.7
D519 OD2	R142 NH1	3.1
K526 N	E141 OE1	2.9
K526 NZ	C132 O	3.1
K526 NZ	E141 O	3.2
Van der Waals		
DT Atom	HBEGF Atom	Distance (Å)
A430 CB	L127 CD2	4.0
L433 CD1	S131 CB	3.7
L433 CD1	I133 CD1	3.9
I464 CD1	V124 CG2	4.0
V468 CG2	I133 CD1	3.9
F470 CD1	V124 CG1	3.9
F470 CE1	L127 CD1	3.9
F470 CZ	L127 CD1	3.9
L512 CD1	L127 CD1	3.7
N524 OD1	L127 CD1	3.7
F530 CE2	G137 CA	3.8
Water-Mediated		
DT Atoms	HBEGF Atoms	Water Molecule
S506 OG; D507 N, OD1; S508 OG	C134 O; H135 O	1
S508 OG; S528 OG	Y138 O	2
S528 OG; K526 O	G140 N	3
K526 O	E141 OE1	4
N524 N; N524 OD1	P130 O	5
S505 O	I133 O	6

upon receptor binding by a DT molecule through its R domain, the unassociated C and T domains are free to carry out their distinct functions. Indeed, as discussed further below, these two domains in the DT–HBEGF complex are swung away from the R domain into an "open" conformation (Figure 2A).

For HBEGF, the bulk of the intermolecular interface

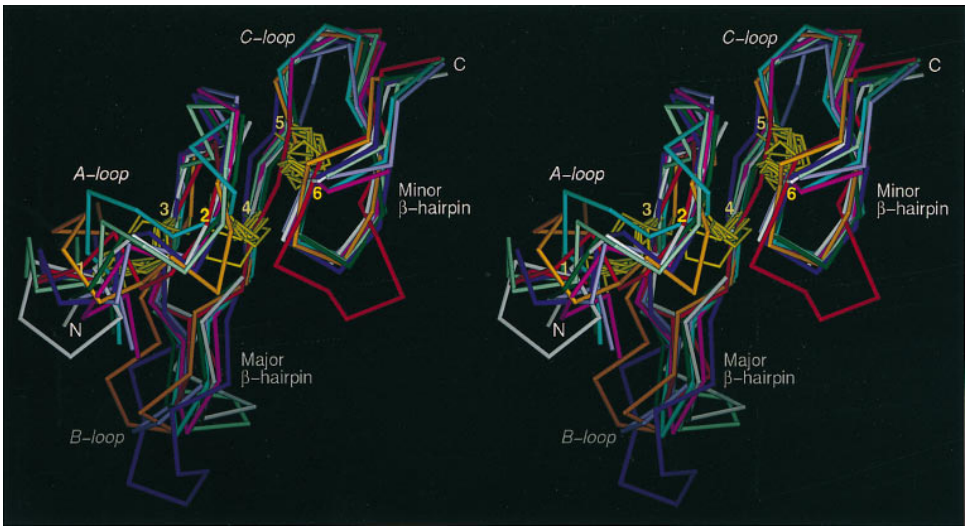

Figure 4. Superposition of α-Carbon Backbones of the Known EGF Structures (Stereo View)

The EGFs (and Protein Data Bank codes, if available) are colored as follows: HBEGF, white; α-heregulin (1haf), dark blue; human EGF (Hommel et al., 1992), light green; transforming growth factor α (2tgf), orange; Factor X EGF module 2 (Rao et al., 1995), dark pink; Factor X EGF module 1 (1apo), dark green; Factor X EGF module 2 (1hcg), red; E-selectin EGF (1esl), light blue; prostaglandin synthase EGF (1pth), violet. The other EGF structures were superimposed onto HBEGF on the basis of least-squares fit of the positions of equivalent (closer than 3.5 Å) α carbons. The major structural features of the EGF fold are labeled. The six cysteines that form the three scaffolding disulfide bonds are shown in yellow. The N domain includes residues up to the fourth cysteine, and the C domain residues from the fifth cysteine onward. Mouse EGF (1epg), which is very similar in sequence and structure to human EGF, and four EGF structures (from fibrillin EGF modules 32 and 33 [1emn], tissue plasminogen activator [Smith et al., 1995], and urokinase [1urk]) that differ more significantly overall (fewer than 30 structurally equivalent α carbons with HBEGF, which have an rms positional deviation greater than 1.7 Å) are excluded from this figure.

with DT is formed by the EGF module; the polypeptide-chain segment of the heparin-binding module (N-terminal to the EGF module, and disordered in the current structure) will likely be directed largely away from the primary interface with DT's R domain (see Figure 2B). This result is consistent with studies on the influence of the heparin-binding module on DT binding. Mitamura et al. (1995) showed from deletion constructs that this module is not absolutely required for binding. Shisido et al. (1995) found that heparin does enhance slightly the binding of DT to HBEGF, but did not observe direct interaction between DT alone and heparin. However, in the DT–HBEGF complex, the heparin-binding region of HBEGF may become juxtaposed with a region of similar function on DT, as the open conformation of the DT molecule exposes a local concentration of basic side chains (K445, K447, H449, R455, K456, R458, R460, K474, H488, H492) on the left-rear face of DT's R domain (see Figures 2A and 3B). This region, the P site, has been shown to function in phosphate binding (Lory et al., 1980).

HBEGF Conformation

The three-dimensional structures of a number of EGF modules have been determined, both as isolated units and as portions of a larger protein. The polypeptide chain of HBEGF in the DT–HBEGF complex has the typical EGF fold, a long and short β hairpin stabilized by three disulfide bonds (Campbell and Bork, 1993). A superposition of HBEGF with a number of other known structures of EGF modules is shown in Figure 4. The conformations and relative orientation of the major and minor β hairpins, the hydrogen-bonding pattern within the hairpins, and the conformations of the reverse turns and of the three disulfide bonds are generally all in good agreement. Like TGF-α, HBEGF has a one-residue deletion in the reverse turn preceding the first β strand, but this deletion causes only a small, local perturbation in the conformation of the polypeptide chain. The largest structural differences among the various EGFs occur within the N-terminal A loop (between the first and second cysteines), and around the B loop reverse turn that links the two strands of the major β hairpin. The overall root-mean-square (rms) positional deviation of equivalent α carbons between HBEGF and the other EGF modules is typically 1.2–1.5 Å for 31–38 residues and is 1.26 Å for 35 residues for α-heregulin (Jacobsen et al., 1996), the EGF structure with the greatest sequence similarity to HBEGF.

The strong structural similarity between HBEGF in the complex and other EGF modules both in solution and in crystals has two implications. First, the R domain of the DT molecule has been adapted to bind HBEGF such that little distortion occurs relative to the uncomplexed form of the receptor. Second, other EGF modules will make feasible recognition targets for engineered DTs with redesigned binding specificities.

Correlation of the Crystal Structure with Other Studies of the DT–HBEGF Interaction

The complex structure explains the effects on receptor binding of a number of modifications of DT. The C terminus (S535) of the DT polypeptide chain is 20 Å distant and directed away from the interface with HBEGF, consistent with the observation that C-terminal extensions

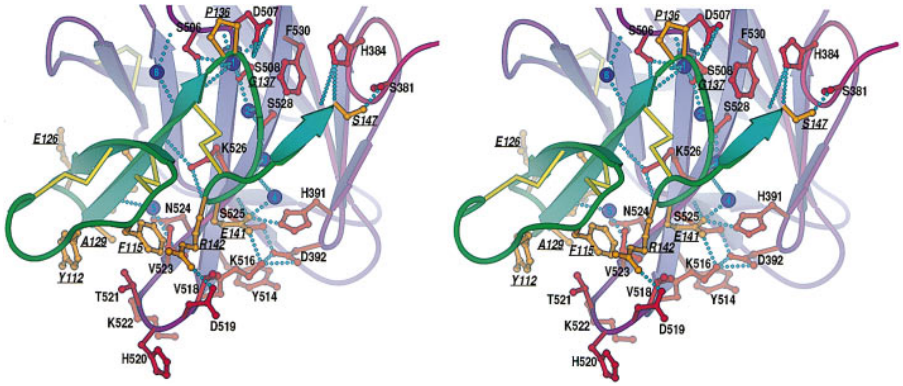

Figure 5. Interactions between DT and HBEGF in the Vicinity of the DT's Rβ9-β10 Loop (Stereo View)

The polypeptide-chain backbones are represented as in Figure 2B. Side chains are colored red for DT and orange for HBEGF. Six water molecules that form bridging interactions between DT and HBEGF are drawn as dark blue spheres. Hydrogen-bond interactions are shown as blue dotted lines.

of 1–12 residues do not interfere with receptor binding (Stenmark et al. 1992). The consequences of C-terminal truncations of DT can also be readily understood. The short deletion of only four residues (after F531) has little effect. On the other hand, truncation after K526, which deletes a key residue (F530) that contacts HBEGF, completely abolishes binding. Additionally, the C-terminal peptide containing residues 482–535, which corresponds to the last three β strands of DT and contains nine side chains that interact with HBEGF, was shown to inhibit competitively binding of the toxin to the receptor (Rolf et al., 1990).

Greenfield et al. (1987) reported two serine-to-phenylalanine substitutions in DT that inhibited receptor binding, S508F (by 100-fold) and S525F (by 8000-fold). S508 is located within the DT–HBEGF interface, although it does not form direct contacts with HBEGF. However, replacement with the bulkier phenylalanine side chain would create steric clashes with HBEGF's C134–C143 disulfide bond and also displace two bound water molecules that interface with HBEGF (see Figure 5). In the space normally occupied by the side chain of S525, a phenylalanine side chain cannot be accommodated and would necessarily cause local structural perturbations in the DT molecule. These perturbations would disrupt the conformation of a number of nearby groups that interact with HBEGF, including the amide nitrogen of K526, and the side chains of H391 and K516.

Shen et al. (1994) have used alanine mutagenesis to investigate the participation in receptor recognition of the solvent-exposed residues in DT's Rβ9-β10 region. Their measurements of the cytotoxicity (which is correlated with the ability to bind to the receptor) of these mutants are in good agreement with the crystal structure. Y514, H520, K522, and S525 form no contacts with HBEGF (Figure 5), and except for Y514, their replacement with alanine had minimal effect on cytotoxicity. The 3.2-fold lower activity of the Y514A mutant may reflect a role of the Y514 side chain in stabilizing the conformation of the Rβ9-β10 hairpin. V518 and V523 form part of a hydrophobic pocket for HBEGF-F115, and also pack against DT-K516 and HBEGF-E141, two residues that form a key interaction in the complex (see below). Their alanine mutants show 2.3-fold and 5.5-fold lower cytotoxicity, respectively. Similarly, T521 makes Van der Waals contacts with HBEGF-Y112 and HBEGF-F115, although its replacement by alanine was shown to have little effect. The loss of two water molecules that are hydrogen-bonded to both S528 and polar groups on HBEGF (Y138 O and G140 N) may explain the 1.9-fold reduced activity of the S528A mutant. N524 forms Van der Waals contacts with HBEGF-L127 and K526 hydrogen bonds HBEGF's C132 O and E141 O, and both side chains are also involved in water-mediated contacts with HBEGF. Alanine replacements of these residues cause 3.3- and 6.1-fold reductions in cytotoxicity, respectively. Van der Waals contacts made by F530 with HBEGF-G137 are important in closing off one end of the interface between the two molecules; the void created by an alanine substitution is likely responsible for the 9.6-fold and 100-fold reductions in cytotoxicity and receptor-binding affinity, respectively. And most notably, the 22-fold and 500-fold decreases in these measures seen in the K516A mutant demonstrate the significance of the interactions formed by K516, as detailed in Figures 3A and 5.

Mouse HBEGF, which is not recognized by DT, differs from the human or monkey forms at ten sites within the EGF module. The effects of these amino acid replacements can be assessed from simple modeling of the substitutions onto the structure of the complexed human HBEGF. Residues 125 and 135 face away from the DT molecule, and thus substitutions at these positions are unlikely to affect binding. The other substitutions do occur at the interface, and curiously, all involve replacement by a larger side chain. Two (K122R and S147T) can likely be accommodated, whereas four others (F115Y, V124L, L127F, and A129T) are certain to create at least some steric conflicts. The I133K substitution places a longer, more polar side chain into the predominantly nonpolar interior of the DT–HBEGF interface. However, the Lys side chain could possibly reorient toward the periphery of the interface and form hydrogen bonds with polar groups of DT-D467. Clearly, the most detrimental substitution is expected to be E141H, which would potentially place three basic side chains (H141 and DT's

H391 and K516) in close proximity in the complex (see Figure 5). Two further observations underscore the importance of interactions formed at the site of this substitution. First, as described above, the K516A mutant shows the largest decreases in toxicity and receptor-binding affinity of any DT mutant studied (Shen et al., 1994). Second, chimeras of mouse HBEGF with either the human or monkey forms show that the single amino acid substitution E141H is sufficient to preclude almost all DT binding (Mitamura et al., 1995). Furthermore, cells expressing monkey HBEGF with this site-directed mutation are 100-fold less sensitive to the toxin and have 12-fold reduced DT affinity relative to cells expressing wild-type HBEGF (Hooper and Eidels, 1996). Nevertheless, binding determinants besides E141 are also important, as mouse HBEGF with the single "humanizing" H141E mutation shows only slight binding to DT.

In summary, measures of the binding capacity of mutants of both DT and HBEGF are consistent with the structure of the DT–HBEGF complex. Furthermore, these other studies are important as they supplement the crystal structure in identifying critical determinants in the DT receptor interaction, and provide additional foundation for redesigning the binding specificity of the toxin.

Conformational Adjustments in DT and a Model for the Interaction of DT with the Membrane Surface

The R domain in the complex makes very little structural adjustment upon binding HBEGF; it differs from the uncomplexed domain in monomeric and dimeric DT by 1.4 and 1.1 Å, respectively (rms positional deviation between corresponding main-chain atoms). The largest structural differences occur at a number of side chains that form direct contacts with the HBEGF molecule and at several loops that surround the binding crevice (Figure 6A). In particular, steric interactions by V468 with HBEGF-I133, and F470 with HBEGF-V124, and salt bridge interactions by R462 with HBEGF-E126, and D465 and D467 with HBEGF-K122 (see Table 1) displace outward the loop containing residues 462–470. The base of this loop is anchored by a disulfide bond (C461–C471). Similarly, interactions with HBEGF centered around D507 and S508 reposition a segment of DT spanning residues 500–508, and this movement appears to affect the position of a neighboring loop containing residues 435–439. In addition, the polypeptide chain at the tip of the Rβ9-β10 hairpin (residues 516–522) shifts inward to position a hydrophobic pocket closer to the side chain of HBEGF-F115. Interestingly, these loops with altered positions in complexed DT apparently have inherent flexibility, as they also show conformational differences between the two uncomplexed monomeric and dimeric forms of DT.

Although only minor structural changes occur within the R domain as a consequence of HBEGF binding, there is an unexpectedly large movement of the domain as a whole. This movement corresponds to the conversion of the complexed DT molecule from a closed to an open conformation. In the DT–HBEGF complex, pairs of open DT molecules associate to form a compact dimer. This dimer is identical to that present in crystals of uncomplexed DT in the dimeric form. Also identical is the conformation of the hinge segment, which dictates the position of the R domain. The similarity between a DT molecule in the complexed and uncomplexed dimeric form is evident in the rms positional deviation of their main-chain atoms, which is 1.0 Å overall, and only slightly lower (0.82 Å) after independent superposition of each of the three domains.

The finding that DT in the complex crystals is in the dimeric form is surprising, as initially, the starting material for forming the complex was monomeric DT. (After the discovery of the DT dimer in the complex crystals, our subsequent crystallization trials with complex formed from dimeric DT that had been isolated by gel-exclusion chromatography yielded identical crystals.) It has been shown previously that DT's monomeric form is the more stable, and conversion to the dimeric form requires very specific conditions (e.g., acidification caused by freezing in mixed phosphate buffer) (Carroll et al., 1986; Fujii et al., 1991). It is not immediately clear how HBEGF induces the DT molecule to dimerize. However, based on the DT–HBEGF structure, a likely explanation is suggested by the close proximity of the C terminus of the HBEGF fragment to DT's hinge segment. Specifically, the backbone carboxylate forms a salt bridge with the side chain of DT-H384, and S147 OG hydrogen bonds DT-S381 OG. The intact HBEGF precursor would have the potential to form even more extensive interactions with the hinge segment, and these interactions may promote a transition to DT's open form. A DT molecule in the open conformation can be trapped in various stable, multimeric forms, and it is the dimeric form that is most amenable to crystallization (Fujii et al., 1991).

A specific interaction between the HBEGF linker and DT hinge segment would explain the seemingly inconsistent previous observation that the dimeric form of DT lacks receptor-binding activity (Carroll et al., 1986). An important distinction is that the earlier studies measured DT binding to intact receptor on cells, whereas the form of HBEGF used in our crystallization experiments is truncated at S147 and lacks the 14-residue linker preceding the transmembrane anchor. In fact, a slightly extended form of HBEGF containing two additional C-terminal residues (148 and 149) fails to yield good crystals of the complex, possibly because the extra residues conflict with the hinge conformation present in the dimeric form of DT. These results suggest that the HBEGF linker passes toward the back face of the R domain, as this path would direct it not only near the hinge segment, but also through the dimer interface (see Figure 2A), and it is for this reason that the DT dimer is unable to bind intact HBEGF.

Because the current structure of the DT–HBEGF complex lacks the HBEGF linker and transmembrane anchor, and the individual domains of DT possess considerable potential for independent movement, the orientation of the DT molecule with respect to the membrane surface cannot be predicted precisely. However, from the available data, we can speculate on a plausible model. A key aspect of this model is that interaction between the linker and DT's hinge induces the DT molecule to adopt an open conformation. Notably, DT in this form has been

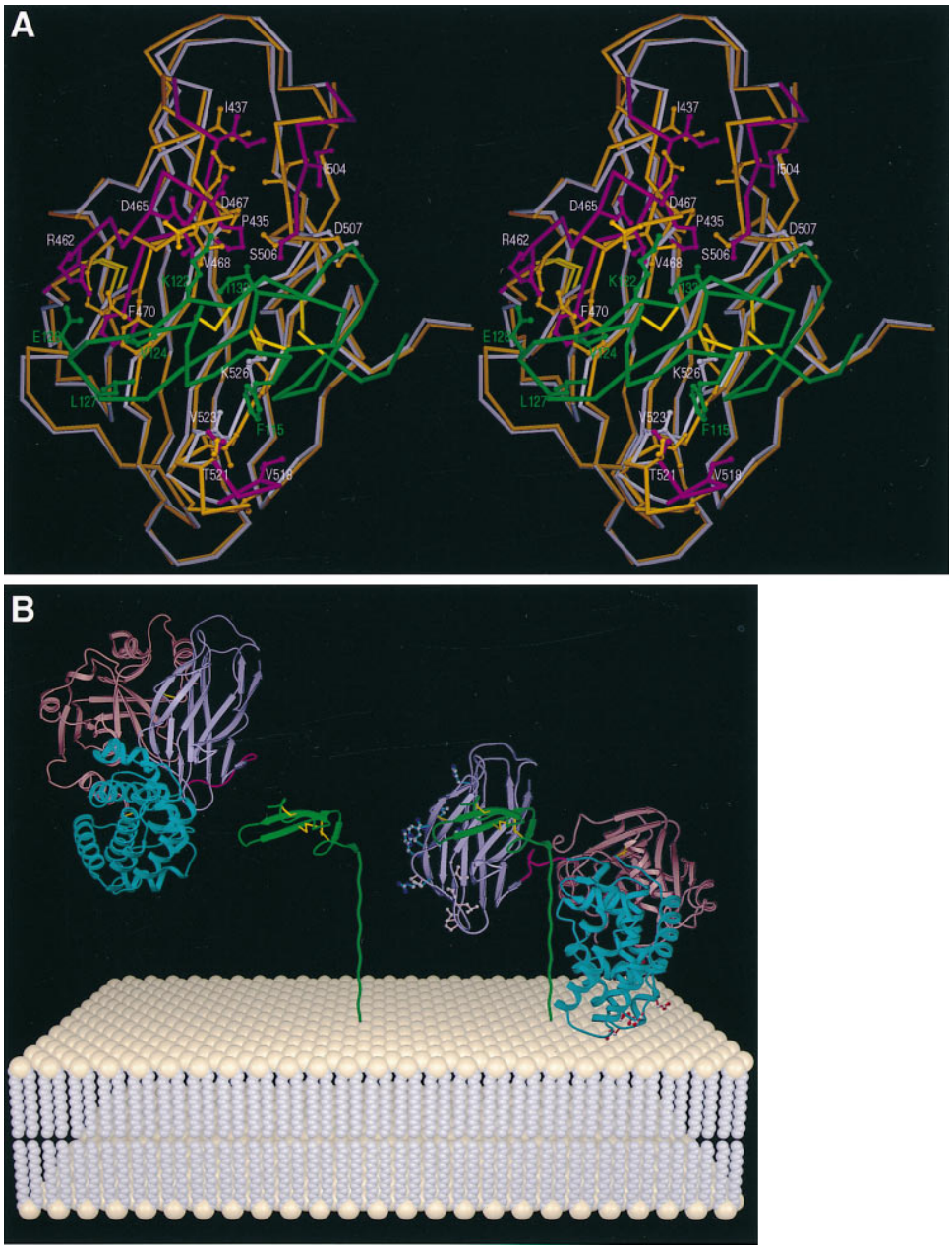

Figure 6. Structural Differences between Complexed and Uncomplexed DT

(A) Comparison of HBEGF-complexed and uncomplexed DT's R domains (stereo view). The α-carbon backbones of the R domain from the DT–HBEGF complex (gray-violet) and dimeric DT (PDB 1ddt, orange) were superimposed on the basis of the positions of all α carbons in residues 387–535. The α-carbon backbone of HBEGF is shown in green. Purple indicates the segments of polypeptide chain of complexed DT with the greatest structural perturbations (residues 435–439, 460–470, 500–506, and 517–521). Amino acid side chains forming intermolecular interactions that appear to be associated with these perturbations are also shown.

(B) A model for the opening of a closed DT molecule (left) upon binding to the HBEGF receptor (green), and the proposed orientation of the open, complexed DT molecule (right) with respect to the membrane surface. Polypeptide chains are represented as in Figure 2. The linker between the HBEGF's EGF module and transmembrane anchor is represented as a fully extended chain ~40 Å in length.

suggested to be an intermediate in the membrane-insertion process (Bennett and Eisenberg, 1994). With the 14 residues of the HBEGF linker fully extended, the EGF module and the membrane surface could potentially be sufficiently separated (~40 Å) to sandwich the bound R domain. The R domain is then appropriately oriented for two regions on its back face to interact with the lipid bilayer: the P-site cluster of basic residues (suggested to form a binding site for phospholipid head groups); and an adjacent, surface-exposed patch of aliphatic side chains (P426-Leu-Pro-Ile-A430, P476, and V483; Bennett et al., 1994) (see Figure 6B). Such interactions may explain the finding that the R domain penetrates the bilayer during membrane translocation (Tortorella et

Table 2. Statistics of the Data Set Used for Refinement of the DT–HBEGF Complex

Resolution Range (Å)	Completeness (%)	Redundancy	Average I/σ (I)	R_{merge}
24.0–5.69	83.3	3.89	50.1	0.029
5.69–4.52	88.4	4.04	48.8	0.038
4.52–3.95	89.3	3.95	45.8	0.043
3.95–3.59	89.7	3.88	34.6	0.063
3.59–3.34	89.7	3.72	25.9	0.063
3.34–3.14	90.0	3.64	18.8	0.070
3.14–2.98	91.5	3.54	13.6	0.090
2.98–2.85	91.9	3.47	10.4	0.110
2.85–2.74	92.0	3.35	7.7	0.135
2.74–2.65	79.2	2.10	5.0	0.152
24.0–2.65	88.5	3.58	27.9	0.052

al., 1995). Furthermore, the loop connecting the TH8 and TH9 helices in the T domain has been suggested to be involved in the acid-pH triggered membrane insertion (Choe et al., 1992). The protonation of acidic side chains on this loop is thought to promote the insertion of these two hydrophobic helices into the endosomal membrane (O'Keefe et al., 1992). With DT's R domain bound to the HBEGF precursor as suggested above and with the DT molecule in an open conformation resembling that observed in the crystal structure, the T domain is suitably oriented for these insertion elements to interact with the membrane. Moreover, the hydrophobic TH9 helix immediately preceding DT's hinge segment has been demonstrated to adopt a transmembrane orientation upon insertion of the T domain into a bilayer (Oh et al., 1996). It is tempting to speculate that interaction between the hinge segment and HBEGF's linker brings this helix into association with the transmembrane helical anchor of the HBEGF precursor. Our postulated roles of the membrane-anchoring segment of HBEGF in fixing the appropriate orientation of the DT molecule and participating in membrane insertion are consistent with the inhibited activity of DT on cells bearing HBEGF with an altered membrane anchor (Lanzrein et al., 1996). Replacement with either a glycosylphosphatidylinositol attachment signal or the transmembrane anchor of an unrelated protein inhibited both the translocation of the DT's C domain and the formation of an ion-conducting channel by the T domain.

Implications for Other EGF Receptor Interactions

The structure determination of the DT–HBEGF complex is the first for an EGF module bound to a specific receptor and may provide a more general model for other EGF–protein interactions. Intriguingly, the amino acid sequence of the EGF receptor predicts a substantially β structure (Ward et al., 1995), thus raising the possibility that EGF and the EGF receptor employ a similar mode of association as both HBEGF with DT and the EGF module with a fibronectin module in t-PA (Smith et al., 1995). A number of site-directed mutagenesis studies have characterized the involvement of residues on EGF in receptor binding. These results suggest that the nonpolar face of the EGF β hairpin that interacts with DT is also critical for binding to the EGF receptor (Richter et al., 1995). In particular, a number of aliphatic side chains in this region of EGF are thought to make hydrophobic contacts with the receptor (Koide et al., 1994, and references therein); in HBEGF, the equivalent residues, V124, L127, and S131, serve this function in the interaction with DT.

Several additional residues that have been demonstrated by substitution experiments to be important in binding of EGF to EGF receptor are involved in key interactions between HBEGF and DT. The phenyl ring of the A-loop F115 fits into a pocket from DT formed by a hairpin that protrudes from the face of the β sheet. The side chain of the adjacent R142 makes two hydrogen bonds to carbonyl groups of D114 and F115 that may stabilize the relative positions of the major and minor β hairpins (Jacobsen et al., 1996), and also forms a direct salt bridge with DT-D519. I133 at the "hinge" between the N and C domains is located at the edge of the nonpolar interface with DT, and interacts with DT-L433 and V468; both polar and nonpolar side chains occur at this site in other EGFs (Puddicombe et al., 1996).

Another notable residue is G137, which is absolutely conserved in the EGFs and is the third residue in a type-I reverse turn. It is involved in two interactions with DT that are dependent on the presence of a glycine at this position. First, the Cα atom makes a Van der Waals interaction with the side chain of F530. Second, the amide nitrogen forms a bifurcated hydrogen bond with the side-chain carboxylate of D507. The appropriate orientation of the peptide bond containing this amide nitrogen is possible only because the glycine permits a type-I turn.

Table 3. Molecular Replacement Solution for DT Portion of DT–HBEGF Complex

Search	Parameters		Best Solution		Peak Height	Next Highest Peak
Rotation function	8.0–3.2 Å, integration radius = 30 Å	α = 58.82°	β = 56.74°	γ = 33.53°	13.7	7.5
Translation function	8.0–3.2 Å	*u* = 0.3483	*v* = 0.3515	*w* = 0.3829	CC = 0.327 R = 0.484	CC = 0.237 R = 0.511

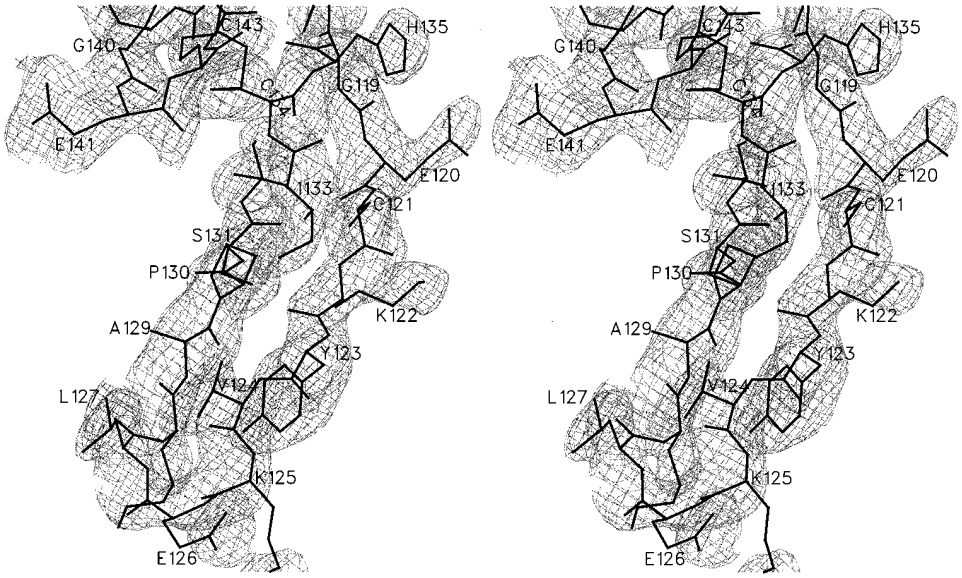

Figure 7. Representative Electron Density from a Simulated-Annealing $F_o - F_c'$ Omit Map Contoured at 1.6 σ

All atoms of HBEGF were omitted in the calculation of structure factors F_c'. The region shown is the major β hairpin of HBEGF.

Experimental Procedures

Source of Proteins

Diphtheria toxin was purchased from Connaught Laboratories (Willowdale, Ontario, Canada). The crude protein was further purified first by DEAE-Sepharose (Pharmacia) ion-exchange chromatography. Subsequent Superdex 75 (Pharmacia) gel-exclusion chromatography yielded monomeric and dimeric forms of DT. The protein fractions were eluted in 25 mM Tris–HCl (pH 7.5), 0.15 M NaCl, 1 mM EDTA, and stored at −20°C.

For the expression of HBEGF in E. coli, the coding region for an extracellular fragment of the protein (containing the heparin-binding and EGF-like modules, residues R73 through S147 of the full-length protein) was subcloned from the plasmid pNA53 (Cook et al., 1995; provided by J. Abraham, Scios Nova, Mountain View, CA). After amplication by polymerase chain reaction, this region was inserted between the NdeI and BamHI sites of the expression vector pET28a (Novagen). The HBEGF protein with a hexahistidine tag at its N terminus was produced in BL21 cells (Novagen). It was initially purified under denaturing conditions (8 M urea) by Ni-NTA Sepharose (Qiagen) chromatography. Then, from a dilute protein solution (0.1 mg/ml) and in the presence of reduced/oxidized glutathione (2.0/0.2 mM), the HBEGF was refolded by dialytic removal of urea in 4, 2, 1, and 0 M urea steps. After thrombin cleavage to remove the hexahistidine tag, the refolded HBEGF was concentrated and further purified by heparin-Sepharose (Pharmacia) chromatography.

The resolution of native and misfolded protein in the HBEGF preparation relied on the inability of the misfolded form to bind DT. DT was combined with a saturating (see below) amount of the HBEGF preparation, and the complex of DT with native HBEGF was separated by gel exclusion (SigmaChrom GFC1300) from misfolded HBEGF. The complex fractions were concentrated and exchanged into 10 mM Tris–HCl (pH 7.5), 0.15 M NaCl by ultrafiltration (Amicon), and used in crystallization trials as described below.

Measurement of Binding Stoichiometry

Two analytical methods were useful for separating the DT and HBEGF proteins in complex from the isolated components. Isoelectric-focusing electrophoresis was run in 5% acrylamide (3% C) gels that contained 5% glycerol and ampholytes with pIs in the range 3–10 (BioRad). Native electrophoresis was run in 4.5% acrylamide (2.7% C) gels containing 0.375 M Tris–HCl (pH 8.8), with electrode buffer containing glycine/Tris (pH 8.3).

Crystallization

Crystals were obtained by vapor diffusion in hanging drops. The protein solution contained a 1:1 mixture of DT and HBEGF at 15–30 mg/ml in 0.15 M NaCl, 10 mM Tris HCl (pH 7.5). The precipitant solution consisted of 22%–30% (w/v) polyethylene glycol 3350 (J. T. Baker), 2.0 M NaCl, 5% (v/v) glycerol, and 50 mM Tris–HCl (pH 7.5). Typically 1 μl volumes of the protein and precipitant solutions were mixed and equilibrated against 1 ml of precipitant. Crystals grew at 23°C over a period of 1–4 weeks to a maximum size of 0.2 × 0.15 × 0.15 mm. Denaturing polyacrylamide electrophoresis on the dissolved crystals confirmed that they contained both proteins. The crystals belong to space group $C222_1$ and have unit-cell dimensions a = 89.4, b = 103.7, and c = 127.7 Å. They contain one DT–HBEGF complex per asymmetric unit and have a calculated solvent content of 45%.

Our structural analysis of the DT–HBEGF crystals has shown that they are related to those of dimeric DT: the crystal packing contacts formed within the a-b plane are nearly identical in the two crystal forms. However, contacts between these planes are entirely different. In particular, these contacts involve the active-site loop (residues 39–45), which is disordered in the complex. This loop has been shown to be affected by the binding of NAD or substrate analogs (Bell and Eisenberg, 1996). It is likely for this reason that the DT–HBEGF complex could be crystallized only if the substrate analog adenylyl-(3′,5′)-uridine 3′-monophosphate was excluded.

X-Ray Data Collection

For X-ray data collection, crystals were mounted in 0.1 mm diameter nylon loops (Hampton Research) and flash frozen in a 100 K nitrogen gas stream (Oxford Cryosystems). Prior to freezing, crystals were immersed briefly in reservoir solution containing 20% (v/v) glycerol as cryoprotectant. X-ray data were measured on a MacScience DIP2000 image-plate system. Incident X-rays from a copper rotating anode, mounted on an M18X generator operated at 50 kV/90 mA, were nickel-filtered and focused with platinum-coated mirrors. The intensity data were integrated and reduced with the programs DENZO and SCALEPACK (Z. Otwinowski and W. Minor), and subsequent manipulation of the data used programs from the Collaborative Computing Project No. 4 suite (1994). The quality of the data set used for the final refinement is detailed in Table 2.

Structure Determination and Refinement

The DT–HBEGF structure determination was initiated with a molecular replacement search for the position and orientation of the DT

portion of the complex. With the atomic coordinates of the entire monomeric DT structure (Bennett and Eisenberg, 1994; entry 1MDT in the Protein Data Bank) as the search model, the program AMoRe (Navaza, 1994) identified a single clear solution (Table 3). The DT molecule was then refined with the program X-PLOR (Brünger, 1992), with a random 5% of the reflections excluded in the test set. First the entire molecule and then each individual domain was treated as a rigid body. After further positional and simulated-annealing refinement and small manual adjustments to the DT portion of the atomic model, $F_{obs} - F_{calc}$ difference electron density located adjacent to one face of a β sheet in the R domain became interpretable. With the known fold of an epidermal-growth-factor module as a guide, a preliminary model for a portion of HBEGF (residues 115–141) was built as a polyalanine skeleton. Then, side chains were assigned and added, and the polypeptide-chain backbone was extended to include residues 110–147. In subsequent refinement steps of the DT–HBEGF complex, a bulk solvent correction was applied, individual atomic temperature factors were refined with tight restraints, and a small number of water molecules were added. Manual inspection of the atomic model against electron-density maps was performed with the program FRODO (Jones, 1985).

The final model includes residues 1–38, 45–188, and 200–535 of DT, residues 107–147 of HBEGF (4308 protein atoms in total), and 48 water molecules. Not included in the atomic model are residues 39–44 and 189–199 of DT, and residues of the heparin-binding module of HBEGF (residues 73–106). These are not visible in electron-density maps and are presumably disordered. With all measured data in the resolution range 24–2.65 Å (15511 reflections in total), the final crystallographic R factors are 0.172 for the working set and 0.290 for the test set. The final model agrees well with ideal stereochemistry (the rms deviations from ideal values are 0.009 Å for bond distances, and 1.5° for bond angles). 87.5% of the residues have most favored backbone phi/psi angles, and none have a disallowed conformation (Laskowski et al., 1993). The atomic temperature factors differ by 4.3 $Å^2$ rms for all bonded atoms, and the average values are 37.5 $Å^2$ for the DT molecule (25.8 $Å^2$ for the R domain alone) and 41.6 $Å^2$ for the HBEGF molecule. The relatively high values for the latter may reflect in part less than full occupancy of the HBEGF portion of the complex. The quality of the electron-density maps is shown in Figure 7.

Acknowledgments

G. V. L. was partly sponsored by a Medical Research Council Canada postdoctoral fellowship. This work was funded in part by the UC Breast Cancer Program and the Breast Cancer Research Program of the US Army. S. C. is indebted to Profs. D. Eisenberg and R. J. Collier for support during the initial stages of this project. We thank members of the Salk Structural Biology Laboratory for helpful discussion, and Dr. Judith Abraham for providing protein samples and expression vectors for HBEGF. Preliminary X-ray data were collected at the Stanford Synchrotron Radiation Laboratory.

Received August 14, 1997; revised September 22, 1997.

References

Bell, C.E., and Eisenberg, D. (1996). Crystal structure of diphtheria toxin bound to nicotinamide adenine dinucleotide. Biochemistry *35*, 1137–1149.

Bennett, M.J., and Eisenberg, D. (1994). Refined structure of monomeric diphtheria toxin at 2.3 Å resolution. Prot. Sci. *3*, 1464–1475.

Bennett, M.J., Choe, S., and Eisenberg, D. (1994). Refined structure of dimeric diphtheria toxin at 2.0 Å resolution. Prot. Sci. *3*, 1444–1463.

Brunger, A.T. (1992). X-PLOR version 3.1: a system for X-ray crystallography and NMR (New Haven, CT: Yale University Press).

Campbell, I.D., and Bork, P. (1993). Epidermal growth factor-like modules. Curr. Opin. Struct. Biol. *3*, 385–392.

Carroll, S.F., Barbieri, J.T., and Collier, R.J. (1986). Dimeric form of diphtheria toxin: purification and characterization. Biochemistry *25*, 2425–2430.

Choe, S., Bennett, M.J., Fujii, G., Curmi, P.M. G., Kantardjieff, K.A., Collier, R.J., and Eisenberg, D. (1992). The crystal structure of diphtheria toxin. Nature *357*, 216–222.

Chothia, C., and Janin, J. (1981). Relative orientation of close-packed β-pleated sheets in proteins. Proc. Natl. Acad. Sci. USA *78*, 4146–4150.

Cook, P.W., Damm, D., Garrick, B., Ashton, N., Wood, K., Karkaria, C.E., Higashiyama, S., Klagsbrun, M., and Abraham, J.A. (1995). Carboxyl-terminal truncation of leucine76 converts heparin-binding EGF-like growth factor from a heparin-enhancible to a heparin-suppressible growth factor. J. Cell. Physiol. *163*, 407–417.

Collier, R.J. (1975). Diphtheria toxin: mode of action and structure. Bacteriol. Rev. *39*, 54–85.

Collaborative Computational Project No. 4. (1994). The CCP4 suite: programs for protein crystallography. Acta Crystallogr. *D50*, 760–763.

Evans, S.V. (1993). SETOR: hardware-lighted three-dimensional solid model representations of macromolecules. J. Mol. Graph. *11*, 134–138.

Fujii, G., Choe, S., Bennett, M.J., and Eisenberg, D. (1991). Crystallization of diphtheria toxin. J. Mol. Biol. *222*, 861–864.

Garcia, K.C., Degano, M., Stanfield, R.L., Brunmark, A., Jackson, M.R., Peterson, P.A., Teyton, L., and Wilson, I.A. (1996). An αβ T cell receptor structure at 2.5 Å and its orientation in the TCR–MHC complex. Science *274*, 209–219.

Greenfield, L., Johnson, V.G., and Youle, R.J. (1987). Mutations in diphtheria toxin separate binding from entry and amplify immunotoxin selectivity. Science *238*, 536–539.

Higashiyama, S., Lau, K., Besner, G.E., Abraham, J.A., and Klagsbrun, M. (1992). Structure of heparin-binding EGF-like growth factor. J. Biol. Chem. *267*, 6205–6212.

Hommel, U., Harvey, T.S., Driscoll, P.C., and Campbell, I.D. (1992). Human epidermal growth factor. High resolution solution structure and comparison with human transforming growth factor alpha. J. Mol. Biol. *227*, 271–282.

Hooper, K.P., and Eidels, L. (1996). Glutamic acid 141 of the diphtheria toxin receptor (HB-EGF precursor) is critical for toxin binding and toxin sensitivity. Biochem. Biophys. Res. Commun. *220*, 675–680.

Jacobsen, N.E., Abadi, N., Sliwkowski, M.X., Reilly, D., Skelton, N., and Fairbrother, W.J. (1996). High-resolution solution structure of the EGF-like domain of heregulin-α. Biochemistry *35*, 3402–3417.

Jones, T.A. (1985). Interactive computer graphics: FRODO. Meth. Enzymol. *115*, 157–171.

Jones, E.Y., Harlos, L., Bottomley, M.J., Robinson, R.C., Driscoll, P.C., Edwards, R.M., Clements, J.M., Dudgeon, T.J. and Stuart, D.I. (1995). Crystal structure of an integrin-binding fragment of vascular cell adhesion molecule-1 at 1.8 Å resolution. Nature *373*, 539–544.

Koide, H., Yokoyama, S., Katayama, Y., Muto, Y., Kigawa, T., Kohno, T., Takusari, H., Oishi, M., Takahashi, S., Tsukumo, K., et al. (1994). Receptor-binding affinities of human epidermal growth factor variants having unnatural amino acid residues in position 23. Biochemistry *33*, 7470–7476.

Lanzrein, M., Sand, O., and Olsnes, S. (1996). GPI-anchored diphtheria toxin receptor allows membrane translocation of the toxin without detectable ion channel activity. EMBO J. *15*, 725–734.

Laskowski, R.A., MacArthur, M.W., Moss, D.S., and Thornton, J.M. (1993). PROCHECK: a program to check the stereochemical quality of protein structures. J. Appl. Crystallogr. *26*, 283–291.

Lory, S., Carroll, S.F., and Collier, R.J. (1980). Ligand interactions of diphtheria toxin: relationships between the NAD site and the P site. J. Biol. Chem. *255*, 12016–12019.

Mitamura, T., Higashiyama, S., Taniguchi, N., Klagsbrun, M., and Mekada, E. (1995). Diphtheria toxin binds to the epidermal growth factor (EGF)-like domain of human heparin-binding EGF-like growth factor/diphtheria toxin receptor and inhibits specifically its mitogenic activity. J. Biol. Chem. *270*, 1015–1019.

Naglich, J.G., Metherall, J.E., Russell, D.W., and Eidels, L. (1992).

Expression cloning of diphtheria toxin receptor: identity with a heparin-binding EGF-like growth factor precursor. Cell *69*, 1051–1061.

Navaza, J. (1994). AMoRe: an automated package for molecular replacement. Acta Crystallogr. *A50*, 157–163.

Nicholls, A., Sharp, K.A., and Honig, B. (1991). Protein folding and association: insights from the interfacial and thermodynamic properties of hydrocarbons. Proteins *11*, 281–296.

O'Keefe, D.O., Cabiaux, V., Choe, S., Eisenberg, D., and Collier, R.J. (1992). pH-dependent insertion of proteins into membranes: B chain mutation of diphtheria toxin that inhibits membrane translocation, Glu349-Lys. Proc. Natl. Acad. Sci. USA *89*, 6202–6206.

Oh, K.J., Zhan, H., Cui, C., Hideg, K., Collier, R.J., and Hubbell, W.L. (1996). Organization of diphtheria toxin T domain in bilayers: a site-directed spin labeling study. Science *273*, 810–812.

Pastan, I., Chaudhary, V., and Fitzgerald, D.J. (1992). Recombinant toxins as novel therapeutic agents. Annu. Rev. Biochem. *61*, 331–354.

Puddicombe, S.M., Chamberlin, S.G., MacGarvie, J., Richter, A., Drummond, D.R., Collins, J., Wood, L., and Davies, D.E. (1996). Significance of valine 33 as a ligand-specific epitope of transforming growth factor α. J. Biol. Chem. *271*, 15367–15372.

Rao, Z., Handford, P., Mayhew, M., Knott, V., Brownlee, G.G., and Stuart, D. (1995). The structure of a Ca^{2+}-binding epidermal growth factor–like domain. Cell *82*, 131–141.

Richter, A., Drummond, D.R., MacGarvie, J., Puddicombe, S.M., Chamberlin, S.G., and Davies, D.E. (1995). Contribution of the transforming growth factor α B-loop β-sheet to binding and activation of the epidermal growth factor receptor. J. Biol. Chem. *270*, 1612–1616.

Rolf, J.M., Gaudin, H.M., and Eidels, L. (1990). Localization of the diphtheria toxin receptor-binding domain to the carboxyl-terminal Mr $\sim$6000 region of the toxin. J. Biol. Chem. *265*, 7331–7337.

Shen, H.S., Choe, S., Eisenberg, D., and Collier, R.J. (1994). Participation of lysine 516 and phenylalanine 530 of diphtheria toxin in receptor recogntion. J. Biol. Chem. *269*, 29077–29084.

Shishido, Y., Sharma, K.D., Higashiyama, S., Klagsbrun, M., and Mekada, E. (1995). Heparin-like molecules on the cell surface potentiate binding of diphtheria toxin receptor/membrane-anchored heparin-binding epidermal growth factor–like growth factor. J. Biol. Chem. *270*, 29578–29585.

Smith, B.O., Downing, A.K., Driscoll, P.C., Dudgeon, T.J., and Campbell, I.D. (1995). The solution structure and backbone dynamics of the fibronectin type I and epidermal growth factor–like pair of modules of tissue-type plasminogen activator. Structure *3*, 823–833.

Stenmark, H., Ariansen, S., Afanasiev, B.N., and Olsnes, S. (1992). Interactions of diphtheria toxin B-fragment with cells. J. Biol. Chem. *267*, 8957–8962.

Sweeney, E.B., and Murphy, J.R. (1995). Diphtheria toxin-based receptor-specific chimeric toxins as targeted therapies. Essays Biochem. *30*, 119–131.

Thompson, S.A., Higashiyama, S., Wood, K., Pollitt, N.S., Damm, D., McEnroe, G., Garrick, B., Ashton, N., Lau, K., Hancock, N., et al. (1994). Characterization of sequences within heparin-binding EGF-like growth factor that mediate interaction with heparin. J. Biol. Chem. *269*, 2541–2549.

Tortorella, D., Sesardic, D., Dawes, C.S. and London, E. (1995). Immunochemical analysis shows all three domains of diphtheria toxin penetrate across model membranes. J. Biol. Chem. *270*, 27446–27452.

Ward, C.W., Hoyne, P.A., and Flegg, F.H. (1995). Insulin and epidermal growth factor receptors contain the cysteine repeat motif found in the tumor necrosis factor receptor. Proteins *22*, 141–153.

Yamaizumi, M., Mekada, E., Uchida, T., and Okada, Y. (1978). One molecule of diphtheria toxin fragment A introduced into a cell can kill the cell. Cell *15*, 245–250.

Zhan, H., Oh, K.J., Shin, Y.-K., Hubbell, W.L., and Collier, R.J. (1995). Interaction of the isolated transmembrane domain of diphtheria toxin with membranes. Biochemistry *34*, 4856–4863.

Protein Data Bank Accession Number

The atomic coordinates for the DT–HBEGF complex have been deposited in the Protein Data Bank under entry number 1XDT.